Comparative Study of Epicatechin–Phenylalanine and Epicatechin–Alanine Interactions Using Quantum Chemistry Methods

ABSTRACT

Aims: This research aims to analyze the interactions within Epicatechin…Phenylalanine complexes and compare them to those in Epicatechin…Alanine complexes through theoretical chemistry calculations.

Methodology: The interactions between Epicatechin and Phenylalanine, an amino acid, are evaluated using theoretical chemistry methods. Calculations performed at the DFT/B3LYP/6-31+G(d,p) level are used to characterize the complexes and their individual monomers. Geometric, energetic, and spectroscopic parameters, along with QTAIM (Quantum Theory of Atoms in Molecules), NBO (Natural Bond Orbital), and NCI (Non-Covalent Interaction) topological analyses, provide insights into the nature and type of these interactions.

Results: The interaction energies of Epicatechin-Phenylalanine complexes exceed those of Epicatechin-Alanine complexes. Unlike the Epicatechin-Alanine complexes, the formation of Epicatechin-Phenylalanine complexes is non-spontaneous. NBO analysis reveals that Epicatechin-Alanine complexes exhibit a greater number of interactions compared to Epicatechin-Phenylalanine complexes, including repulsive interactions attributed to the phenyl group. Moreover, the total stabilization energies of Epicatechin-Phenylalanine complexes are higher than those of their Catechin-Alanine and Epicatechin-Alanine counterparts.

Conclusion: The non-covalent bonds formed in epicatechin-phenylalanine complexes are stronger and more numerous than those in catechin-alanine and epicatechin-alanine complexes.

Keywords: Polyphenols , Epicatechin, Catechin, DFT, QTAIM, NBO, NCI

1. INTRODUCTION

Plants produce numerous secondary metabolites, including terpenoids, alkaloids, and polyphenols. Polyphenols are present in all parts of plants (roots, stems, flowers, leaves). They are found in the composition of the most common consumer products, particularly fruits and vegetables, as well as derived products like chocolate, tea, and red wine. [1–4]. By consuming these food products, humans benefit from antioxidant properties[5–9] notably delaying cell aging and combating certain chronic diseases, including cardiovascular and neurodegenerative diseases [5, 6, 10–12]. Polyphenols are highly reactive compounds.

Indeed, once in the body, polyphenols interact with the compounds present there. These interactions lead to the formation of more or less stable complexes. Several studies, particularly the theoretical studies conducted on epicatechin…alanine complexes, have shown that the interactions occurring in these complexes are non-covalent. The main non-covalent interactions are moderate hydrogen bonds with a partially covalent character [13]. The effects of the presence of other groups in the structure of alanine, particularly the phenyl group, could help to better understand the interactions between polyphenols and proteins. This research aims to identify the interactions that occur within the epicatechin…phenylalanine complexes and then compare them with those that take place in the epicatechin…alanine complexes [13], using theoretical chemistry calculations at the DFT level with the B3LYP functional and the 6-31+G (d, p) basis set. This study also combines NBO (Natural Bond Orbital) and QTAIM (Quantum Theory of Atoms in Molecules) calculations to account for electronic displacements within molecules as well as the formation of intermolecular hydrogen bonds that reflect the stabilization of structures.

2. MATERIAL AND METHODS

The structures of epicatechin, phenylalanine, and alanine used in this study are represented in Figure 1. Phenylalanine is distinguished from alanine by the presence of a phenyl group in its structure. Figure 2 presents the epicatechin…phenylalanine complexes. These complexes are formed by the proximity of the hydroxyl group O28-H29, which is one of the most reactive hydroxyl groups of epicatechin [14] ,and the heteroatoms Nsp3, Osp2, and Osp3 of phenylalanine.

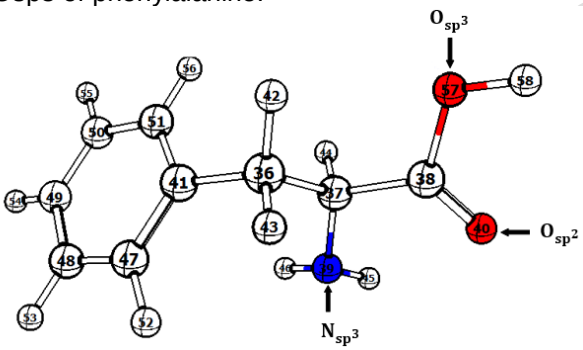

Phenylalanine

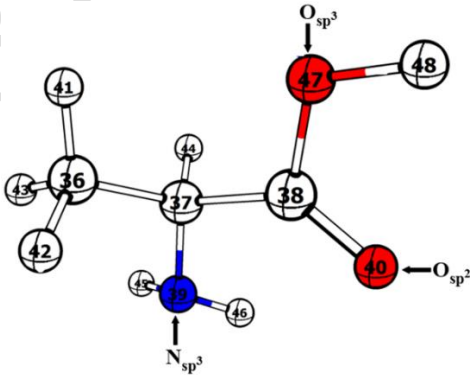

Alanine

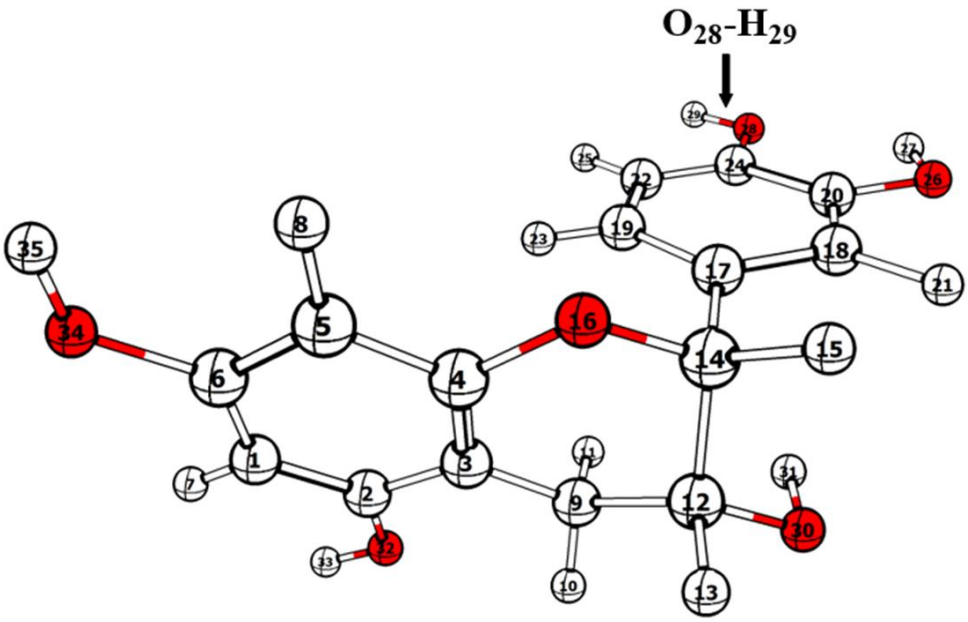

Epicatechin

Figure 1: Structures of epicatechin, alanine and phenylalanine.

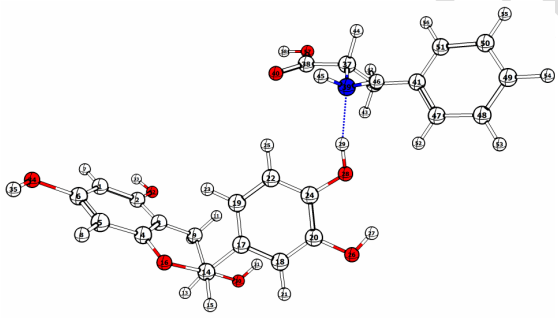

Complexe Epicat $\mathbf{O_{28} - H_{29}} \cdots$ Phe Nsp^3

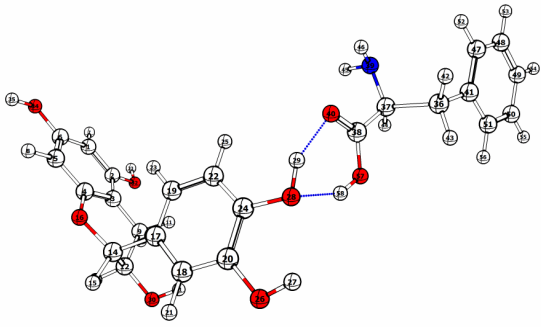

Complexe Epicat $\mathbf{O_{28} - H_{29}} \cdots$ Phe Osp^2

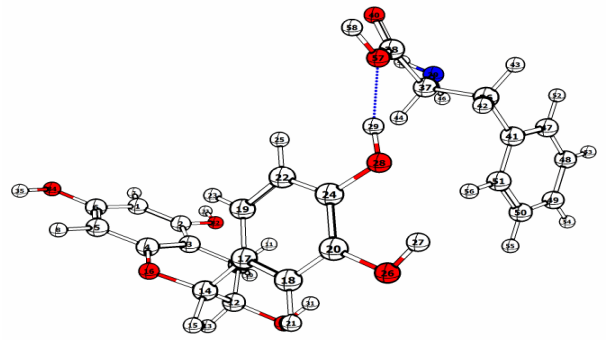

Complexe Epicat $\mathbf{O_{28} - H_{29}}$ ··· Phe Osp3

Figure 2 : Optimised structures of the complexes Epicat $\mathbf{O_{28} - H_{29}}$ ··· Phe Nsp^3, Epicat $\mathbf{O_{28} - H_{29}}$ ··· Phe Osp^2 and Epicat $\mathbf{O_{28} - H_{29}}$ ··· Phe Osp3.

These structures were optimised at the b3lyp/6-31+G(d,p) level of theory using Gaussian 09 ref software in order to approximate the ground state structure. The optimised structures were subjected to frequency calculations and various quantum chemical analyses. The frequency calculations were used to determine the spectroscopic and thermodynamic parameters, in particular the interaction energy of each complex. This interaction energy is refined by the ZPE (Zero-Point Energy) and the BSSE (Basis Set Superposition Error). [15, 16]. NBO (Natural Bond Orbital) analysis is used to determine electron delocalisation between atoms in the same molecule or between atoms in different molecules. It is used to list intermolecular interactions, assess their energy and identify the main interactions in the complex formed. QTAIM analysis is used to identify the interactions taking place in the complex, to determine their nature and to establish the strength of the hydrogen bonds. The NCI analysis specifies attractive interactions, repulsive interactions (steric hindrances) and van der Waals interactions.

2.1 Standard Enthalpy of Formation and Standard Gibbs Free Energy of Formation

The standard enthalpy of formation ΔH_f^0 and the standard free enthalpy of formation ΔG_f^0 are used to assess the exothermicity and spontaneity of the reaction to form a molecule, respectively. Conversely, these values can be used to characterise the relative stability of a series of molecules. These two thermodynamic quantities, ΔH_f^0 and ΔG_f^0 are determined according to the formulae of Ochterski et al. [17].

2.2 Interaction Energy

The interaction energy was determined after an optimisation followed by a frequency calculation. This energy represents the difference between the total energy of the complex and the energies of the monomers. To determine the interaction energy, the ZPE (Zero-Point Energy) and the BSSE (Basis Set Superposition Error) are used to correct the excessive stabilisation of the complex [15, 16, 18]. In the complex, each molecular orbital is developed in a larger base than that of the monomers, which leads to excessive stabilisation of the complex. The expression for the interaction energy E_(int) then becomes :

$$\mathbf{E_{int} = E_{complex} - \sum E_{monomers} + E_{BSSE} + \Delta ZPE}$$

With

$$\mathbf{\Delta ZPE = ZPE^{complex} - \sum ZPE^{monomers}}$$

2.3 NBO Analysis

NBO (Natural Bond Orbital) analysis is a technique used to determine the charge transfer properties of molecules. It offers a comprehensive insight into the nature of intra- and intermolecular orbital interactions, with a particular focus on hydrogen bonds (both intra- and intermolecular) between occupied NBO donors and empty NBO acceptors [19, 20] . A charge transfer is the movement of electrons from an electron donor site (Lewis-type orbital: Lone pair (LP), natural bond (σ and π)) to an electron acceptor site (anti-Lewis orbital: : σ^* and π^*). The electron delocalisation is accompanied by a decrease in the electron density of the donor and an increase in the electron density of the acceptor. This occurs when a lone pair (LP), natural bond (σ and π) is transferred to an electron acceptor site (anti-Lewis orbital : σ* and π*). The stabilisation energy E^2 is used to evaluate the electron delocalisation i → j :

$$E^{(2)} = \Delta E_{ij} = q_i \frac{F^2(i,j)}{\varepsilon_j - \varepsilon_i}$$

Where q_i is the electron density in the donor orbital, F (i,j) is a non-diagonal element of the Fock matrix , ε_i et ε_j are the energies of the occupied i and vacant j orbitals respectively.

The higher the $E^{(2)}$, the more stable the redistribution of electrons between the donor and acceptor.

2.4. AIM Topological Analysis

Bader's Quantum Theory of Atoms in Molecules (QTAIM) is a highly useful method for the topological analysis of chemical bonds [21, 22]. In this theory, the presence of chemical bonds between two atoms or interatomic interactions is determined by the existence of a bond critical point (BCP).The characteristics of bond critical points allow the description of the covalent or non-covalent nature of intermolecular interactions, particularly hydrogen bonds. The most commonly used characteristics of bond critical points include the electron density ρ(r) and its Laplacian $\nabla^2(\rho(r))$, the total electronic energy density H(r), the potential electronic energy density V(r), and the kinetic energy density G(r). These parameters enable the classification of hydrogen bonds based on their strength. According to the work of Rozas et al. [23], the following classification is established at different bond critical points: For strong hydrogen bonds $\nabla^2(\rho)<0$, $H(r)<0$; For medium hydrogen bonds $\nabla^2(\rho)>0$, $H(r)<0$; For weak hydrogen bonds $\nabla^2(\rho)>0$, $H(r)>0$. The ratio $-\frac{G(r)}{V(r)}$ is also used to determine the nature of the interaction at different BCPs [24]. When $-\frac{G(r)}{V(r)}>1$, the bond is considered non-covalent. If $0,5<\frac{G(r)}{V(r)}<1$ the bond exhibits partial covalent character. For $\frac{G(r)}{V(r)}<0,5$ the bond is purely covalent. The energy of the hydrogen bond is evaluated using the relation $E_{HB}=-\frac{1}{2}V(r)$ according to the work of Espinosa [25].

2.5. NCI Analysis

NCI (Non-Covalent Interaction) Analysis is a theoretical method used to study and characterize non-covalent interactions. This analysis highlights the distinction between attractive interactions (hydrogen bonds), repulsive interactions (steric effects), and Van der Waals (VDW) interactions [26, 20, 27]. Through a 3D graphical visualization of NCI isosurfaces, different interactions are represented by specific colors: blue for hydrogen bonds, green for Van der Waals interactions, and red for repulsive interactions. Additionally, a 2D graphical representation of the reduced density gradient as a function of sign $(\lambda_2) \times \rho(r)$, helps associate each type of interaction with its corresponding region [27, 20, 26] . Peaks appearing in regions where sign $(\lambda_2) \times \rho(r) < 0$ correspond to attractive interactions (hydrogen bonds) ; signe $(\lambda_2) \times \rho(r) = 0$ indicates Van der Waals interactions ; sign $(\lambda_2) \times \rho(r) > 0$ is associated with repulsive interactions.

3. RESULTS AND DISCUSSION

This section presents the obtained results and their corresponding interpretations.

3.1. Thermodynamic Parameters and Interaction Energy

The thermodynamic parameters and interaction energy values of the complexes Epicatechin ... Phenylalanine and Epicatechin ... Alanine are summarized in Table 1. The complexation enthalpy (ΔH) values for the complexes $EpicatO_{28}$-$H_{29}\cdots PheN_{sp^3}$, $EpicatO_{28}$-$H_{29}\cdots PheO_{sp^2}$ and $EpicatO_{28}$-$H_{29}\cdots PheO_{sp^3}$ range from -11.09 to -4.11 kcal/mol. These values are higher than those for the complexes $EpicatO_{28}$-$H_{29}\cdots AlaN_{sp^3}$, $EpicatO_{28}$-$H_{29}\cdots AlaO_{sp^2}$ et $EpicatO_{28}$-$H_{29}\cdots AlaO_{sp^3}$ which range from -19,30 to -14.83 kcal/mol[13]. These results indicate that

the formation of these complexes is exothermic. However, the formation of Epicatechin ... Phenylalanine complexes is less exothermic than that of Epicatechin ... Alanine complexes. Among the Epicatechin ... Phenylalanine complexes, $\mathrm{EpicatO_{28}-H_{29}\cdots PheN_{sp^3}}$ is more exothermic compared to $\mathrm{EpicatO_{28}-H_{29}\cdots PheO_{sp^2}}$ and $\mathrm{EpicatO_{28}-H_{29}\cdots PheO_{sp^3}}$. The same trend is observed for the *Epicatechin ... Alanine* complexes, where EpicatO_{28}-H_{29}···AlaN_{sp^3} is more exothermic than EpicatO_{28}-H_{29}···AlaO_{sp^2} and EpicatO_{28}-H_{29}···AlaO_{sp^3}.

The free enthalpy of complexation (ΔG) values for EpicatO_{28}-H_{29}···PheN_{sp^3}, EpicatO_{28}-H_{29}···PheO_{sp^2} and EpicatO_{28}-H_{29}···PheO_{sp^3} are positive , whereas those for EpicatO_{28}-H_{29}···AlaN_{sp^3}, EpicatO_{28}-H_{29}···AlaO_{sp^2} and EpicatO_{28}-H_{29}···AlaO_{sp^3} are negative [13]. These values suggest that the interactions between *Epicatechin* and *Phenylalanine* are non-spontaneous under the calculated conditions, whereas the interactions between *Epicatechin* and *Alanine* are spontaneous. The phenyl group in *Phenylalanine* disrupts the spontaneity of interactions with *Epicatechin*.

The interaction energies for Epicat O_{28}-H_{29}···Phe N_{sp^3}, Epicat O_{28}-H_{29}···Phe O_{sp^2} and Epicat O_{28}-H_{29}···Phe O_{sp^3} complexes are negative, ranging from -10.01 to -3.74 kcal/mol. The ranking of interaction energies with the N_{sp^3} site is as follows : $\mathrm{E_{int}(Epicat\ O_{28}-H_{29}\cdots Phe\ N_{sp^3})} < \mathrm{E_{int}(Epicat\ O_{28}-H_{29}\cdots Phe\ O_{sp^2})} < \mathrm{E_{int}(Epicat\ O_{28}-H_{29}\cdots Phe\ O_{sp^3})}$. These values are higher than those for Epicat O_{28}-H_{29}···Ala N_{sp^3}, Epicat O_{28}-H_{29}···Ala O_{sp^2} and Epicat O_{28}-H_{29}···Ala O_{sp^3}, indicating that the interactions between the hydroxyl group O_{28}-H_{29} of *Epicatechin* and the heteroatoms N_{sp^3}, O_{sp^2} and O_{sp^3} in Phenylalanine are weaker than those with the corresponding heteroatoms in Alanine. The presence of the phenyl group in *Phenylalanine* weakens the complexes Epicat O_{28}-H_{29}···Phe N_{sp^3}, Epicat O_{28}-H_{29}···Phe O_{sp^2} et Epicat O_{28}-H_{29}···Phe O_{sp^3}.

Table 1. Energetic Parameters of the Epicatechin ... Phenylalanine and Epicatechin ... Alanine Complexes Studied

Complexe	**E_{int} (Kcal/mol)**	**ΔH**	**ΔG**
Epicatechin…Phenylalanine			
Epicat $\mathrm{O_{28}-H_{29}\cdots}$ Phe Nsp^3	-10.01	-11.09	0.21
Epicat $\mathrm{O_{28}-H_{29}\cdots}$ Phe Osp^2	-8.82	-9.43	1.12
Epicat $\mathrm{O_{28}-H_{29}\cdots}$ Phe Osp^3	-3.95	-4.38	5.00
Epicatechin…Alanine [13]			
Epicat $\mathrm{O_{28}-H_{29}\cdots}$ Ala Nsp^3	-19.30	-20.12	-10.99

Epicat $O_{28} - H_{29} \cdots$ Ala O_{sp^2}	-18.36	-18.73	-9.19
Epicat $O_{28} - H_{29} \cdots$ Ala O_{sp^3}	-14.83	-14.88	-6.78

The NBO and AIM analyses will determine the nature of the interactions occurring in the complexes Epicat O_{28}-H_{29}···Phe N_{sp^3}, Epicat O_{28}-H_{29}···Phe O_{sp^2} and Epicat O_{28}-H_{29}···Phe O_{sp^3} particularly those influenced by the phenyl group.

3.2. NBO Analysis

The parameters of the NBO analysis are presented in Tables 2 to 7. In the complex Epicat O_{28}-H_{29}···Phe N_{sp^3}, the total stabilization energy $\sum E^{(2)}$is 32.31 kcal/mol, compared to 31.09 kcal/mol in the complex Epicat O_{28}-H_{29}···Ala N_{sp^3}[13]. The interactions present in the Epicat O_{28}-H_{29}···Phe N_{sp^3} complex include the hydrogen bonds O_{28}-H_{29}···N_{39}, C_{22}-H_{25}···O_{40}, C_{47}-H_{52}···O_{28} along with other interactions such as O_{28}-H_{29}···N_{39}-H_{45}, C_{22}-H_{25}···C_{38}=O_{40}. These interactions are more numerous than those found in the Epicat O_{28}-H_{29}···Ala N_{sp^3}. The hydrogen bond O_{28}-H_{29}···N_{39} arises from the electronic delocalization of the nitrogen atom's lone pair N_{39} ($LP^{(1)}_{N39}$) toward the anti-Lewis orbital $\sigma^*_{O28-H29}$. This delocalization is represented by the electronic transition $LP^{(1)}_{N39} \rightarrow \sigma^*_{O28\text{-}H29}$. During this electronic delocalization, 56.28 me of charge is transferred, corresponding to a stabilization energy of 28.64 kcal/mol (88.7 % of $\sum E^{(2)}$) in the Epicat O_{28}-H_{29}···Phe N_{sp^3} complex, compared to 29.9 kcal/mol in the Epicat O_{28}-H_{29}···Ala N_{sp^3} complex. The stabilization energies of the other interactions are relatively low. Hence, the hydrogen bond O_{28}-H_{29}···N_{39} is the primary interaction in both EpicatO_{28}-H_{29}···PheN_{sp^3} and Epicat O_{28}-H_{29}···Ala N_{sp^3}.

Table 2: Stabilization Energies $\mathbf{E^{(2)}}$, Total Stabilization Energies $\sum \mathbf{E^{(2)}}$, and Charge Transfers (CT) of the Complex Epicat O_{28}-H_{29}··· Phe N_{sp^3}

Epicat O_{28}-H_{29}··· Phe N_{sp^3}

Contact	Electronic Transition	$\mathbf{E^{(2)}}$ (kcal/mol)	$\sum \mathbf{E^{(2)}}$ (kcal/mol)	CT (me)
$C_{47} - H_{52} \cdots O_{28}$	$LP^{(1)}_{O28} \rightarrow \sigma^*_{C47-H52}$	0.41		0.60
	$LP^{(2)}_{O28} \rightarrow \sigma^*_{C47-H52}$	0.06		0.11
$C_{36} - H_{43} \cdots O_{28}$	$LP^{(2)}_{O28} \rightarrow \sigma^*_{C36-H43}$	0.20		0.44
$O_{28} - H_{29} \cdots N_{39}$	$LP^{(1)}_{N39} \rightarrow \sigma^*_{O28-H29}$	28.64	32.31	56.38
$C_{22} - H_{25} \cdots O_{40}$	$LP^{(1)}_{O40} \rightarrow \sigma^*_{C22-H25}$	0.77		1.02
	$LP^{(2)}_{O40} \rightarrow \sigma^*_{C22-H25}$	0.47		0.90

C_{22}-H_{25}⋯O_{40}=C_{38}	$\pi_{C38-O40} \rightarrow \sigma^*_{C22-H25}$	0.41		0.67
O_{28}-H_{29}⋯H_{45}-N_{39}	$\sigma_{N39-H45} \rightarrow \sigma^*_{O28-H29}$	0.63		0.93
O_{28}-H_{29}⋯H_{46}-N_{39}	$\sigma_{N39-H46} \rightarrow \sigma^*_{O28-H29}$	0.72		1.01

Table 1 : Stabilization Energies $E^{(2)}$, Total Stabilization Energies $\sum E^{(2)}$ and Charge Transfers (CT) of the Complex Epicat O_{28}-H_{29}⋯ Ala N_{sp^3} [13]

Epicat $O_{28} - H_{29} \cdots$ Ala N_{sp^3}

Contact	Electronic Transition	$E^{(2)}$ (kcal/mol)	$\sum E^{(2)}$ (kcal/mol)	CT (me)
$O_{28} - H_{29} \cdots N_{39}$	$LP^{(1)}_{N39} \rightarrow \sigma^*_{O28-H29}$	29.9		56.64
$C_{38} - H_{41} \cdots O_{28}$	$LP^{(1)}_{O28} \rightarrow \sigma^*_{C38-H41}$	0.09		0.16
O_{28}- $H_{29} \cdots H_{44} - C_{37}$	$\sigma_{C37-H44} \rightarrow \sigma^*_{O28-H29}$	0.12	31.09	0.20
O_{28} - $H_{29} \cdots N_{39} - C_{37}$	$\sigma_{C37-N39} \rightarrow \sigma^*_{O28-H29}$	0.36		0.45
O_{28} - $H_{29} \cdots H_{45} - N_{39}$	$\sigma_{N39-H45} \rightarrow \sigma^*_{O28-H29}$	0.62		0.86

The total stabilization energy of the Epicat O_{28}-H_{29}⋯Phe O_{sp^2}, complex is equal to 30.55 kcal/mol (table 4). This energy is 23.97 kcal/mol in the Epicat O_{28}-H_{29}⋯Ala O_{sp^2} complex (table 5). In the Epicat O_{28}-H_{29}⋯Phe O_{sp^2} complex, the interactions observed are O_{28}-H_{29}⋯O_{40} , O_{57}-H_{58}⋯O_{28}, O_{28}-H_{28}⋯O_{40}=C_{38} and O_{28}-H_{29}⋯C_{38}-C_{37}. The hydrogen bond O_{28}-H_{29}⋯O_{40} results from the electronic delocalizations $LP^{(1)}_{O40} \rightarrow \sigma^*_{O28\text{-}H29}$ and $LP^{(2)}_{O40} \rightarrow \sigma^*_{O28\text{-}H29}$. For these two delocalizations, the charge transfers and stabilization energies are 36.16 me and 19.06 kcal/mol respectively. Similarly, the hydrogen bond O_{57}-H_{58}⋯O_{28} is described by two electronic delocalizations : $LP^{(1)}_{O28} \rightarrow \sigma^*_{O57\text{-}H58}$ and $LP^{(2)}_{O28} \rightarrow \sigma^*_{O57\text{-}H58}$. The CT and $E^{(2)}$ values for these electronic delocalizations are 21.32 me and 10.86 kcal/mol respectively. The stabilization energies of the hydrogen bonds O_{28}-H_{29}⋯O_{40} and O_{57}-H_{58}⋯O_{28} account for more than 90% of the total stabilization energy of the EpicatO_{28}-H_{29}⋯PheO_{sp^2} complex. These two hydrogen bonds are the main interactions in the EpicatO_{28}-H_{29}⋯PheO_{sp^2}.

Table 2 : Stabilization Energies $E^{(2)}$, Total Stabilization Energies $\sum E^{(2)}$ and Charge Transfers (CT) of the Complex Epicat O_{28}-H_{29}⋯ Phe O_{sp^2} complex.

Epicat $O_{28} - H_{29} \cdots$ Phe O_{sp^2}

Contact	Electronic Transition	$E^{(2)}$ (kcal/mol)	$\sum E^{(2)}$ (kcal/mol)	CT (me)

$O_{57} - H_{58} \cdots O_{28}$	$LP^{(1)}_{O28} \rightarrow \sigma^*_{O58-H57}$	2.38		3.80
	$LP^{(2)}_{O28} \rightarrow \sigma^*_{O58-H57}$	8.48		17.52
$O_{28} - H_{29} \cdots O_{40}$	$LP^{(1)}_{O40} \rightarrow \sigma^*_{O28-H29}$	5.85	30.55	8.00
	$LP^{(2)}_{O40} \rightarrow \sigma^*_{O28-H29}$	13.21		28.16
$O_{28} - H_{29} \cdots C_{38} - C_{37}$	$\sigma_{C37-C38} \rightarrow \sigma^*_{O28-H29}$	0.24		0.32
$C_{28} - H_{29} \cdots O_{40} = C_{38}$	$\pi_{C38-O40} \rightarrow \sigma^*_{O28-H29}$	0.39		0.41

Table 3 : Stabilization Energies $E^{(2)}$, Total Stabilization Energies $\sum E^{(2)}$ and Charge Transfers (CT) of the ComplexEpicat O_{28}-H_{29}··· Ala O_{sp^2} [13]

Epicat $O_{28} - H_{29} \cdots$ Ala O_{sp^2}

Contact	**Electronic Transition**	$\mathbf{E^{(2)}}$ **(kcal/mol)**	$\sum \mathbf{E^{(2)}}$ **(kcal/mol)**	**CT (me)**
$O_{28} - H_{29} \cdots O_{40}$	$LP^{(1)}_{O40} \rightarrow \sigma^*_{O28-H29}$	8.7		11.31
	$LP^{(2)}_{O40} \rightarrow \sigma^*_{O28-H29}$	11.51		23.11
$N_{39} - H_{46} \cdots O_{28}$	$LP^{(1)}_{O28} \rightarrow \sigma^*_{N39-H46}$	0.64		0.92
	$LP^{(2)}_{O28} \rightarrow \sigma^*_{N39-H46}$	1.81		3.52
$C_{38} - O_{40} \cdots O_{28}$	$LP^{(1)}_{O28} \rightarrow \pi^*_{C38-O40}$	0.1		0.16
$N_{39} - H_{46} \cdots H_{29} - O_{28}$	$\sigma_{O28-H29} \rightarrow \sigma^*_{N39-H46}$	0,28	23.97	0.37
$C_{22} - H_{25} \cdots O_{40}$	$LP^{(1)}_{O40} \rightarrow \sigma^*_{C22-H25}$	0.13		0.17
$O_{28} - H_{29} \cdots O_{40} - C_{38}$	$\sigma_{C38-O40} \rightarrow \sigma^*_{O28-H29}$	0.38		0.38
$C_{22} - H_{25} \cdots O_{40} - C_{38}$	$\pi_{C38-O40} \rightarrow \sigma^*_{C22-H25}$	0.12		0.20
$O_{28} - H_{29} \cdots O_{47} - C_{38}$	$\sigma_{C38-O47} \rightarrow \sigma^*_{O28-H29}$	0.18		0.19
$O_{28} - H_{29} \cdots H_{46} - N_{39}$	$\sigma_{N39-H46} \rightarrow \sigma^*_{O28-H29}$	0.12		0.16

The stabilization energy is 11.59 kcal/mol in the EpicatO_{28}-H_{29}···PheO_{sp^3} complex, compared to 11,86 kcal/mol in the EpicatO_{28}-H_{29}···AlaO_{sp^3} complex (Tables 6 and 7). In the

EpicatO_{28}-H_{29}···PheO_{sp^2} complex, the hydrogen bond O_{28}-H_{29}···O_{57} is characterized by electronic delocalizations $LP^{(1)}_{O57} \rightarrow \sigma^{*}_{O28\text{-}H29}$ and $LP^{(2)}_{O57} \rightarrow \sigma^{*}_{O28\text{-}H29}$. The charge transfers associated with these electronic delocalizations are 16,33 me, and the $E^{(2)}$ value of the hydrogen bond O_{28}-H_{29}···O_{57} is 11.09 $\mathrm{kcal/mol}$ (95.7 % of $\sum E^{(2)}$). The hydrogen bond O_{28}-H_{29}···O_{57} is the main interaction in these complexes. In addition to this primary interaction, other interactions such as C_{36}-H_{42}···O_{28}, C_{22}-H_{25}···O_{57}, C_{51}-H_{43}···O_{28} et C_{37}-H_{44}···C_{19}=C_{22} also occur in this complex.

Table 4. Stabilization Energies $E^{(2)}$, Total Stabilization Energies $\sum E^{(2)}$ and Charge Transfers (CT) of the Complex Epicat O_{28}-H_{29}··· Phe O_{sp^3}

Complexe Epicat O_{28}-H_{29}··· Phe O_{sp^3}				
Contact	**Electronic Transition**	$\mathbf{E^{(2)}}$ $(\mathbf{kcal/mol})$	$\sum \mathbf{E^{(2)}}$ $(\mathbf{kcal/mol})$	**CT** $(\mathbf{me})$
C_{36}-H_{42}···O_{28}	$LP^{(1)}_{O28} \rightarrow \sigma^{*}_{C36-H42}$	0.06	11.59	0.09
	$LP^{(2)}_{O28} \rightarrow \sigma^{*}_{C36-H42}$	0.16		0.33
C_{51}-H_{56}···O_{28}	$LP^{(2)}_{O28} \rightarrow \sigma^{*}_{C51-H56}$	0.17		0.36
O_{28}-H_{29}···O_{57}	$LP^{(1)}_{O57} \rightarrow \sigma^{*}_{O28-H29}$	9.79		13.84
	$LP^{(2)}_{O57} \rightarrow \sigma^{*}_{O28-H29}$	1.30		2.49
C_{22}-H_{25}···O_{57}	$LP^{(1)}_{O57} \rightarrow \sigma^{*}_{C22-H25}$	0.11		0.22

Table 5: Stabilization Energies $E^{(2)}$, Total Stabilization Energies $\sum E^{(2)}$ and Charge Transfers (CT) of the Complex Epicat O_{28}-H_{29}··· Ala O_{sp^3} [13]

$\mathbf{Epicat\ O_{28} - H_{29} \cdots\ Ala\ O_{sp^3}}$				
Contact	**Electronic Transition**	$\mathbf{E^{(2)}}$ $(\mathbf{kcal/mol})$	$\sum \mathbf{E^{(2)}}$ $(\mathbf{kcal/mol})$	**CT** $(\mathbf{me})$
$O_{28} - H_{29} \cdots O_{47}$	$LP^{(1)}_{O47} \rightarrow \sigma^{*}_{O28-H29}$	10.31	11.86	14.43
	$LP^{(2)}_{O47} \rightarrow \sigma^{*}_{O28-H29}$	0.64		1.22
$C_{36} - H_{41} \cdots O_{28}$	$LP^{(2)}_{O28} \rightarrow \sigma^{*}_{C36-H41}$	0.37		0.72

$C_{22} - H_{25} \cdots O_{47}$	$LP_{O47}^{(2)} \rightarrow \sigma^*_{C22-H25}$	0.13	0.22
$C_{38} - O_{47} \cdots H_{29} - O_{29}$	$\sigma_{O28-H29} \rightarrow \sigma^*_{C38-O47}$	0.15	0.21
$O_{28} - H_{29} \cdots H_{41} - C_{36}$	$\sigma_{C36-H41} \rightarrow \sigma^*_{O28-H29}$	0.14	0.20
$O_{28} - H_{29} \cdots H_{47} - O_{48}$	$\sigma_{O48-H47} \rightarrow \sigma^*_{O28-H29}$	0.12	0.15

This analysis indicates that the complexes EpicatO_{28}-H_{29}···PheN_{sp^3}, EpicatO_{28}-H_{29}···PheO_{sp^2} et EpicatO_{28}-H_{29}···PheO_{sp^3} exhibit several interactions of different types. These interactions include: O-H···N, O-H···O, C-H···N, C-H···O, N-H···O, O-H···C=O, C-H···C=O, O-H···C=C, C-H···C=C, N-H···C=C, O-H···H-O, O-H···H-C, O-H···H-N and others. As is the case in the Epicatechin…Alanine complexes, the main interactions in the Epicatechine…Phenylalanine complexes are hydrogen bonds O-H···N, O-H···O ; with the hydrogen bonds involving the Nsp^3 and Osp^2 heteroatoms of Phenylalanine being more intense than those with the Osp^3 site. The total stabilization energies of the Epicatechin…Phenylalanine complexes are higher than those of their Epicatechin…Alanine counterparts. These results are consistent with the structure of Phenylalanine, as its aromatic ring allows for additional interactions with Epicatechin and Catechin.

3.3 Geometric and spectroscopic parameters

Tables 8 and 9 present the geometric and spectroscopic parameters of the hydrogen bonds in the Epicatechin…Phenylalanine and Epicatechin…Alanine complexes studied. In all hydrogen bonding interactions O-H···O, O-H···N et N-H···O, the variations in the lengths of the O-H and N-H groups are positive (Δd(O-H)>0, Δd(N-H)>0). The O-H et N-H groups elongate. Their elongation frequencies decrease ($\Delta\nu(O\text{-}H) < 0$, Δν(N-H)<0). The hydrogen bonds O-H···O, O-H···N et N-H···O in the complexes EpicatO_{28}-H_{29}···PheN_{sp^3}, EpicatO_{28}-H_{29}···PheO_{sp^2} and EpicatO_{28}-H_{29}···PheO_{sp^3} are proper hydrogen bonds. The intermolecular distances and linearity angles of the O-H···O et O-H···N hydrogen bonds range from 1.8 to 1.9 Å and from 139° to 170°, respectively. These intermolecular distances are between 1.5 Å and 2.2 Å, while the linearity angles are between 130º and 180º. Thus, the $O - H \cdots O$, $O - H \cdots N$ hydrogen bonds occurring in Epicatechin...Phenylalanine complexes are medium to moderate hydrogen bonds. For N-H···O hydrogen bonds, intermolecular distances range from 2.18 Å to 2.78 Å, and linearity angles from 94º to 163º. These hydrogen bonds are weak. For the C-H···O and C-H···N interactions, the $C - H$ bond contract (Δd(C-H)<0) while their stretching frequencies increase (Δν(C-H)>0). These interactions are improper or unconventional hydrogen bonds. In addition, for these hydrogen bonds, the intermolecular distances and linearity angles are between 2.52 Å and 3.15 Å and then between 102º and 165º, respectively. These unconventional $C - H \cdots O$ and $C - H \cdots N$ hydrogen bonds are weak.

The intermolecular distances of the hydrogen bonds O_{28}-H_{29}···N_{39}, O_{28}-H_{29}···O_{40} et O_{28}-H_{29}···O_{47} are higher. These bonds have lower linearity angles in the EpicatO_{28}-H_{29}···PheN_{sp^3}, EpicatO_{28}-H_{29}···PheO_{sp^2} and EpicatO_{28}-H_{29}···PheO_{sp^3} complexes than in EpicatO_{28}-H_{29}···AlaN_{sp^3}, EpicatO_{28}-H_{29}···AlaO_{sp^2} and EpicatO_{28}-H_{29}···AlaO_{sp^3} complexes. This indicates the hydrogen bonds of Epicatechin ...Phenylalanine are weaker than those of Epicatechin ...Alanine complexes.

Table 8: Geometric Parameters of X – H ··· Y Interactions (Distance in Å, Angle in Degrees) and Stretching Frequency Shifts ∆υ (cm-1) of X – H Bonds in the Epicatechin ··· Phenylalanine Complexes

Complexes	**Interactions**	**d(H···Y)**	**∠XHY**	**Δd(X−H); Δd(C−H)**	**$\Delta\nu_{X-H}$; $\Delta\nu_{C-H}$**
Epicat O_{28}-H_{29}··· Phe N_{sp^3}	C_{47}-H_{52}···O_{28}	2.76106	140.8	0.71415	29.8
	C_{36}-H_{43}···O_{28}	3.01159	121.5	-0.00089	30.1
	O_{28}-H_{29}···N_{39}	1.80202	169.2	0.03136	-640.8
	C_{22}-H_{43}···O_{40}	2.53187	162.6	-0.00199	28.1
Epicat O_{28}-H_{29}··· Phe O_{sp^2}	O_{57}-H_{58}···O_{28}	1,94960	150.8	0.01051	-200.8
	O_{28}-H_{29}···O_{40}	1.82509	147.1	0.01921	-380.8
Epicat O_{28}-H_{29}··· Phe O_{sp^3}	C_{36}-H_{42}···O_{28}	2.93600	136.3	-0.00368	29.3
	C_{51}-H_{56}···O_{28}	3.05389	150.1	0.00029	-1.3
	O_{28}-H_{29}···O_{57}	1.93723	170.4	0.00738	-145.5
	C_{22}-H_{25}···O_{57}	3.07497	123.4	-0.00103	12.1

Table 6 : Geometric Parameters of X – H ··· Y Interactions (Distance in Å, Angle in Degrees) and Stretching Frequency Shifts ∆υ (cm-1) of X – H Bonds in the Epicatechin ··· Alanine Complexes [13]

Complexes	**Contact**	**d(H···Y)**	**∠XHY**	**Δd(X−H) ; Δd(C−H)**	**$\Delta\nu_{X-H}$; $\Delta\nu_{C-H}$**
Epicat $O_{28} - H_{29} \cdots$ Ala N_{sp^3}	$O_{28} - H_{29} \cdots N_{39}$	1.79761	171.1	0.03092	-634.8
	$C_{36} - H_{41} \cdots O_{28}$	2.96005	123.7	-0.002	92.8
Epicat $O_{28} - H_{29} \cdots$ Ala O_{sp^2}	$O_{28} - H_{29} \cdots O_{40}$	1.80454	168.2	0.01523	-299.1
	$N_{39} - H_{45} \cdots O_{28}$	2.36187	147.3	0.00096	-8.8
	$C_{22} - H_{25} \cdots O_{43}$	2.85709	123.2	-0.00157	20.5
Epicat $O_{28} - H_{29} \cdots$ Ala O_{sp^3}	$O_{28} - H_{29} \cdots O_{47}$	1.93377	172.6	0.00702	-138.7
	$C_{36} - H_{41} \cdots O_{28}$	2.85381	150.7	-0.00274	19.6

$C_{22} - H_{25} \cdots O_{47}$	3.04357	124.2	-0.00103	12.6

AIM molecular graphs of the EpicatO$_{28}$-H$_{29}$···PheN$_{sp^3}$, EpicatO$_{28}$-H$_{29}$···PheO$_{sp^2}$ et EpicatO$_{28}$-H$_{29}$···PheO$_{sp^3}$ complexes are shown in Figure 3. The parameters of the AIM analysis are listed in Tables 10 and 11. The electron densities $\rho(r)$ of the BCPs of the intermolecular contacts established between X-H groups (X = O, N, C) and the Y heteroatoms (Y = Nsp^3, Osp^2 et Osp^3) of Epicatechin and Phenylalanine range from 0,001753 to 0,044983 ea_0^{-3}. The Laplacians $\nabla^2\rho(r)$ of all these interactions are positive. They range from 0.006272 to 0.099029 ea_0^{-5}. The X-H···Y interactions are hydrogen bonds. The total electronic energy densities H(r) of most of the O-H···Y et N-H···Y interactions are negative. Also the ratios $-\frac{G(r)}{V(r)}$, ranging from 0.901 to 0.999, satisfy the criterion $0.5 < -\frac{G(r)}{V(r)} < 1$. The O-H···Y and N-H···Y interactions are moderate hydrogen bonds with partial covalent character. The interaction O$_{28}$-H$_{29}$···O$_{57}$, in the EpicatO$_{28}$-H$_{29}$···PheO$_{sp^3}$ complex has a positive H(r) value, with a $-\frac{G(r)}{V(r)}$ ratio close to 1. This interaction is a moderate hydrogen bond with partial covalent character. . The hydrogen bond energy E_{HB} values range from 5 to 10 kcal/mol. These values confirm that the O-H···Y and N-H···Y contacts are moderate hydrogen bonds because $4\ \text{kcal/mol} < E_{HB} < 15\ \text{kcal/mol}$. The AIM parameters of the C–H…O and C–H…N contacts are such that: $\nabla^2(\rho(r) > 0$, $H(r) > 0$, $-\frac{G(r)}{V(r)} > 1$ et $E_{HB} < 4\ \text{kcal/mol}$. Thus, the C–H···O and C–H···N interactions are classified as weak hydrogen bonds. AIM analysis indicates that the complexes EpicatO$_{28}$-H$_{29}$···PheN$_{sp^3}$, EpicatO$_{28}$-H$_{29}$···PheO$_{sp^2}$ and EpicatO$_{28}$-H$_{29}$···PheO$_{sp^3}$ are formed through moderate hydrogen bonds of the types O – H…Y and N – H…Y alongside which exist weak hydrogen bonds C – H…O and C – H…N. Other weak interactions, including C – N … C = C, C – H … C = C et C – H … H – C, are also present.

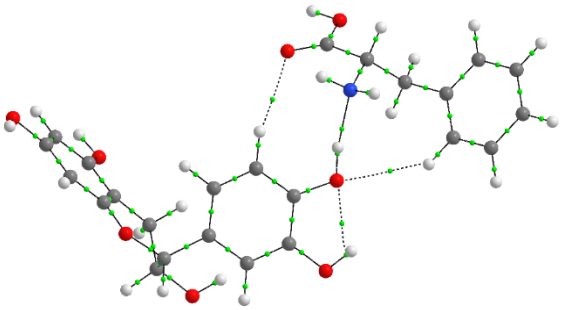

EpicatO$_{28}$-H$_{29}$···PheN$_{sp^3}$

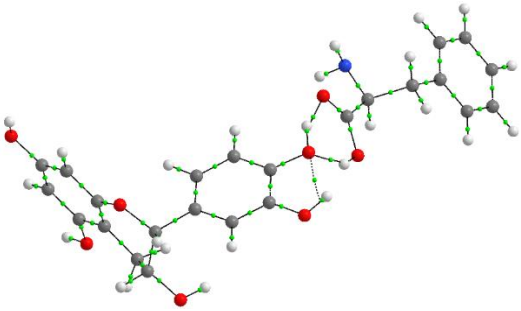

EpicatO$_{28}$-H$_{29}$···PheO$_{sp^2}$

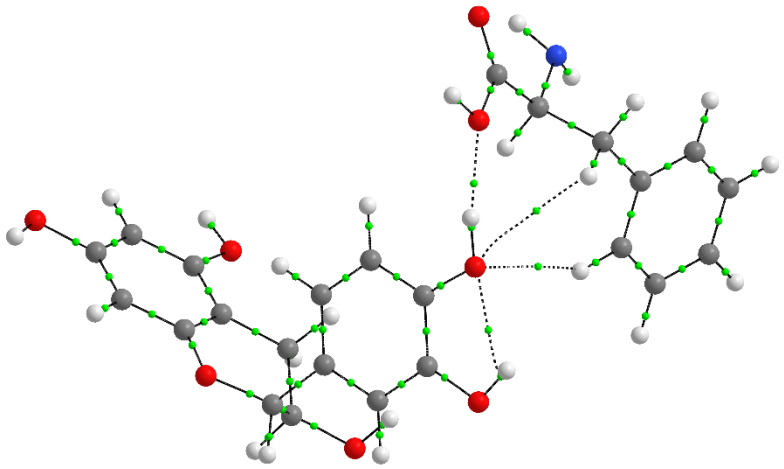

$Epicat O_{28}$-H_{29}···$PheO_{sp^3}$

Figure 3 : AIM Molecular Graphs of the Complexes $Epicat O_{28}$-H_{29}···$PheN_{sp^3}$, $Epicat O_{28}$-H_{29}···$PheO_{sp^2}$ and $Epicat O_{28}$-H_{29}···$PheO_{sp^3}$

Table 10 : Topological Analysis of Bond Critical Points (BCP) of X-H ··· Y Contacts in Epicatechin ··· Phenylalanine Interactions

Contact	$\rho(r)_{X-H\cdots Y}$ (ea_0^{-3})	$\nabla^2\rho(r)_{X-H\cdots Y}$ (ea_0^{-5})	V(r) (u.a.)	G(r) (u.a)	H(r) (u.a.)	$-\frac{G(r)}{V(r)}$	E_{HB}(kcal/mol)
$Epicat O_{28} - H_{29} \cdots PheN_{sp^3}$							
$C_{22} - H_{25} \cdots O_{40}$	0.007749	0.026616	-0.005114	0.005884	0.00077	1.151	1.60
$O_{28} - H_{29} \cdots N_{39}$	0.043047	0.092126	-0.028724	0.025878	-0.002847	0.901	9.01
$C_{47} - H_{52} \cdots O_{28}$	0.004765	0.017933	-0.002862	0.003673	0.000811	1.283	0.90
$Epicat O_{28} - H_{29} \cdots PheO_{sp^2}$							
$O_{28} - H_{29} \cdots O_{40}$	0.034632	0.099029	-0.026296	0.025527	-0.000769	0.971	8.25
$O_{57} - H_{58} \cdots O_{28}$	0.025396	0.070728	-0.019068	0.018375	-0.000693	0.964	5.98
$Epicat O_{28} - H_{29} \cdots PheO_{sp^3}$							
$C_{47} - H_{52} \cdots O_{28}$	0.003825	0.015396	-0.002036	0.002943	0.000906	1.445	0.64
$O_{28} - H_{29} \cdots O_{57}$	0.024092	0.071913	-0.017965	0.017971	0.000007	1.000	5.64
$C_{51} - H_{56} \cdots O_{28}$	0.003055	0.011493	-0.001505	0.002189	0.000684	1.454	0.47

Table 11 : Topological Analysis of Bond Critical Points (BCP) of X-H ⋯ Y Contacts in Epicatechin ⋯ Alanine interaction [13]

Contact	$\rho(r)_{X-H\cdots Y}$ (ea_0^{-3})	$\nabla^2\rho(r)_{X-H\cdots Y}$ (ea_0^{-5})	V(r) (u.a.)	G(r) (u.a)	H(r) (u.a.)	$-\frac{G(r)}{V(r)}$	$E_{HB}(kcal/mol)$
$EpicatO_{28} - H_{29} \cdots AlaN_{sp^3}$							
$O_{28} - H_{29} \cdots N_{39}$	0.043552	0.093384	-0.029193	0.02627	-0.002923	0.900	9.16
$EpicatO_{28} - H_{29} \cdots PheO_{sp^2}$							
$O_{28} - H_{29} \cdots O_{40}$	0.032866	0.101413	-0.024061	0.024707	0.000646	1.027	7.55
$N_{39} - H_{46} \cdots O_{28}$	0.010796	0.036099	-0.007924	0.008474	0.000550	1.069	2.49
$EpicatO_{28} - H_{29} \cdots PheO_{sp^3}$							
$O_{28} - H_{29} \cdots O_{47}$	0.024023	0.072554	-0.017924	0.018031	0.000107	1.006	5.62
$C_{36} - H_{41} \cdots O_{28}$	0.004408	0.017568	-0.002366	0.003379	0.001013	1.428	0.74

3.4 NCI-RDG analysis

The 3D graphical visualization of the NCI isosurfaces and the 2D visualization of the reduced density gradient (RDG) as a function of sign (λ_2) × ρ(r) of the complexes EpicatO_{28}-H_{29}⋯PheN_{sp^3}, EpicatO_{28}-H_{29}…PheO_{sp^2} and EpicatO_{28}-H_{29}⋯PheO_{sp^3} are shown in Figure 4. The 2D visualization of the reduced density gradient (RDG) as a function of sign (λ_2) × ρ(r) reveals peaks at -0,040 a.u.<sign(λ_2)×ρ(r)<-0,010 a.u. These peaks indicate the presence of attractive interactions, in particular hydrogen bonds. The blue colour of the isosurfaces between the hydrogen atoms of the groups O – H, N – H, C – H and the heteroatoms O and N confirm the presence of the hydrogen bonds O-H⋯O, O-H⋯N, C-H⋯O and N-H⋯O. Peaks at 0,010 a.u.<sign(λ_2)×ρ(r)<0,020 a.u. show the presence of repulsive interactions (steric hindrances). These repulsive interactions take place between the O and O atoms, O and N atoms and within the aromatic rings. Red isosurfaces appear between these atoms and within the aromatic rings. In the complex Epicat O_{28}-H_{29}⋯Phe O_{sp^3}, the presence of green isosurfaces reveals the existence of van der Waals (VDW) interactions. The peaks corresponding to these interactions are observed at sign(λ_2)×ρ(r)=0.

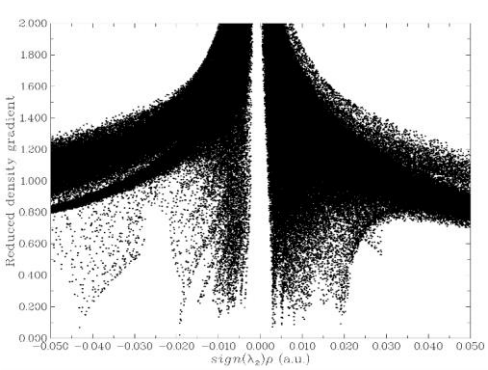

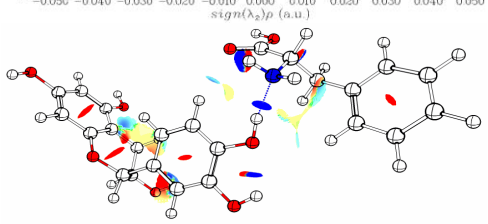

Epicat O_{28}-H_{29}···Phe N_{sp^3}

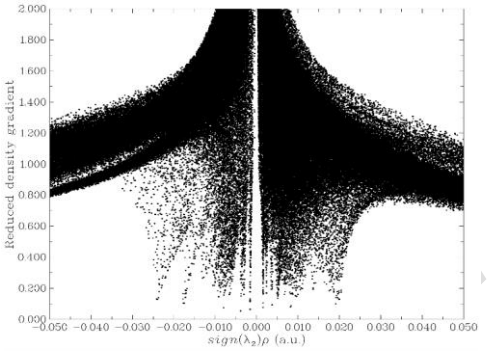

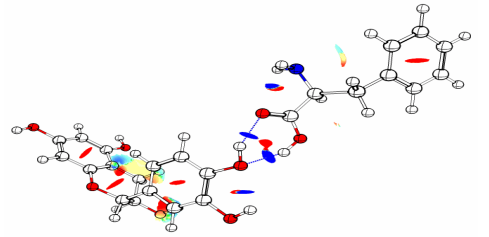

Epicat O_{28}-H_{29}···Phe O_{sp^2}

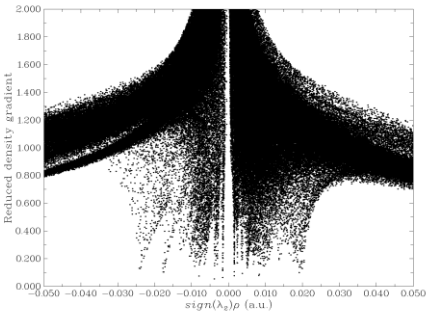

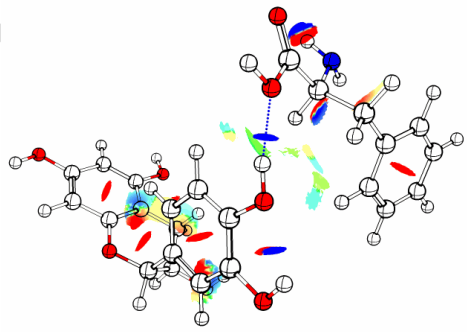

Epicat O_{28}-H_{29}···Phe O_{sp^3}

Figure 4: NCI Isosurface and Reduced Density Gradient (RDG) Plot as a Function of sign(λ_2)×ρ(r) for the Complexes EpicatO_{28}-H_{29}···PheN_{sp^3}, EpicatO_{28}-H_{29}···PheO_{sp^2} and EpicatO_{28}-H_{29}···PheO_{sp^3}

4. CONCLUSION

We performed a detailed theoretical analysis of the complexes EpicatO_{28}-H_{29}···PheN_{sp^3}, EpicatO_{28}-H_{29}…PheO_{sp^2} and EpicatO_{28}-H_{29}···PheO_{sp^3}. The structures of these complexes were optimized, and harmonic frequency analyses were performed. The structure of Phenylalanine is equivalent to that of Alanine, with a hydrogen atom on the β-carbon replaced by a phenyl group. This structural difference is also reflected in the complexes formed. Indeed, the interaction energies of the Epicatechin…Phenylalanine complexes are higher than those of the Epicatechin…Alanine complexes. Additionally, the formation of Epicatechin…Phenylalanine complexes is non-spontaneous, unlike the Epicatechin…Alanine complexes.

The NBO analysis reveals that the interactions in the Epicatechin…Alanine complexes are more numerous than those in the Epicatechin…Phenylalanine complexes, particularly due to repulsive interactions caused by the presence of the phenyl group. The total stabilization energies of the Epicatechin…Phenylalanine complexes are higher than those of their Catechin…Alanine and Epicatechin…Alanine counterparts. However, the stabilization energies of the primary interactions in the homologous complexes are of the same order. Thus, complexes formed with proteins composed of low-molecular-weight amino acids (notably alanine) will be more stable than those formed with proteins composed of high-molecular-weight amino acids or those containing aromatic rings (notably phenylalanine). In contrast to the complexes formed with low-molecular-weight amino acids, those formed with high-molecular-weight proteins are unlikely to be found in large quantities in stools and urine.

Disclaimer (Artificial intelligence)

Option 1:

Author(s) hereby declare that NO generative AI technologies such as Large Language Models (ChatGPT, COPILOT, etc.) and text-to-image generators have been used during the writing or editing of this manuscript.

REFERENCES

1. Terahara N (2015) Flavonoids in Foods: A Review. Natural Product Communications 10:1934578X1501000. https://doi.org/10.1177/1934578X1501000334
2. Snopek L, Mlcek J, Sochorova L et al. (2018) Contribution of Red Wine Consumption to Human Health Protection. Molecules 23. https://doi.org/10.3390/molecules23071684
3. Cantos E, Espín JC, Tomás-Barberán FA (2002) Varietal differences among the polyphenol profiles of seven table grape cultivars studied by LC-DAD-MS-MS. J Agric Food Chem 50:5691–5696. https://doi.org/10.1021/jf0204102
4. Ruidavets J, Teissedre P, Ferrières J et al. (2000) Catechin in the Mediterranean diet: vegetable, fruit or wine? Atherosclerosis 153:107–117. https://doi.org/10.1016/s0021-9150(00)00377-4
5. Hollman PCH, Cassidy A, Comte B et al. (2011) The biological relevance of direct antioxidant effects of polyphenols for cardiovascular health in humans is not established. J Nutr 141:989S-1009S. https://doi.org/10.3945/jn.110.131490
6. Manach C, Mazur A, Scalbert A (2005) Polyphenols and prevention of cardiovascular diseases. Curr Opin Lipidol 16:77–84. https://doi.org/10.1097/00041433-200502000-00013
7. Sugihara N, Ohnishi M, Imamura M et al. (2001) Differences in Antioxidative Efficiency of Catechins in Various Metal-Induced Lipid Peroxidations in Cultured Hepatocytes. JOURNAL OF HEALTH SCIENCE 47:99–106. https://doi.org/10.1248/jhs.47.99
8. Villaño D, Fernández-Pachón MS, Moyá ML et al. (2007) Radical scavenging ability of polyphenolic compounds towards DPPH free radical. Talanta 71:230–235. https://doi.org/10.1016/j.talanta.2006.03.050
9. Preedy VR (2012) Tea in Health and Disease Prevention. Elsevier Science & Technology Books, San Diego, CA, USA
10. Farkhondeh T, Yazdi HS, Samarghandian S (2019) The Protective Effects of Green Tea Catechins in the Management of Neurodegenerative Diseases: A Review. Curr Drug Discov Technol 16:57–65. https://doi.org/10.2174/1570163815666180219115453
11. Grzesik M, Naparło K, Bartosz G et al. (2018) Antioxidant properties of catechins: Comparison with other antioxidants. Food Chem 241:480–492. https://doi.org/10.1016/j.foodchem.2017.08.117
12. Pervin M, Unno K, Ohishi T et al. (2018) Beneficial Effects of Green Tea Catechins on Neurodegenerative Diseases. Molecules 23. https://doi.org/10.3390/molecules23061297
13. Akpa Eugene E, Boka Robert N, Ganiyou A et al. (2023) Modelling Interactions Between Flavanols and Amine Acids: Case of Catechin and Epicatechin with Alanine; NBO, AIM, NCI Analysis. SJC 11:88–107. https://doi.org/10.11648/j.sjc.20231103.13

14. Eugène EA, Robert NB, Ganiyou A et al. (2022) Catechin and Epicatechin. What's the More Reactive? CC 10:53–70. https://doi.org/10.4236/cc.2022.102003
15. Anikina E.V., Beskachko V.P., E.V. A et al. (2020) Basis set superposition error: Effects of atomic basis set optimization on value of counterpoise correction. Вестник Южно-Уральского государственного университета. Серия: Математика. Механика. Физика 12:55–62
16. Boys SF, Bernardi F (1970) The calculation of small molecular interactions by the differences of separate total energies. Some procedures with reduced errors. Molecular Physics 19:553–566. https://doi.org/10.1080/00268977000101561
17. (2000) Thermochemistry in gaussian
18. Boys SF, Bernardi F (2002) The calculation of small molecular interactions by the differences of separate total energies. Some procedures with reduced errors. Molecular Physics 100:65–73. https://doi.org/10.1080/00268970110088901
19. Snehalatha M, Ravikumar C, Hubert Joe I et al. (2009) Spectroscopic analysis and DFT calculations of a food additive carmoisine. Spectrochim Acta A Mol Biomol Spectrosc 72:654–662. https://doi.org/10.1016/j.saa.2008.11.017
20. Venkataramanan NS, Suvitha A (2017) Structure, electronic, inclusion complex formation behavior and spectral properties of pillarplex. J Incl Phenom Macrocycl Chem 88:53–67. https://doi.org/10.1007/s10847-017-0711-y
21. Bader RFW (1990) Atoms in molecules: A quantum theory. International series of monographs on chemistry. Clarendon press, Oxford, New York
22. Bader RFW (1991) A quantum theory of molecular structure and its applications. Chem Rev 91:893–928. https://doi.org/10.1021/cr00005a013
23. Rozas I, Alkorta I, Elguero J (2000) Behavior of Ylides Containing N, O, and C Atoms as Hydrogen Bond Acceptors. J Am Chem Soc 122:11154–11161. https://doi.org/10.1021/ja0017864
24. Ziółkowski M, Grabowski SJ, Leszczynski J (2006) Cooperativity in hydrogen-bonded interactions: ab initio and "atoms in molecules" analyses. J Phys Chem A 110:6514–6521. https://doi.org/10.1021/jp060537k
25. Espinosa E, Molins E, Lecomte C (1998) Hydrogen bond strengths revealed by topological analyses of experimentally observed electron densities. Chemical Physics Letters 285:170–173. https://doi.org/10.1016/S0009-2614(98)00036-0
26. Chakraborty D, Chattaraj PK (2018) Confinement induced thermodynamic and kinetic facilitation of some Diels-Alder reactions inside a CB7 cavitand. Journal of Computational Chemistry 39:151–160. https://doi.org/10.1002/jcc.25094
27. Venkataramanan NS, Suvitha A, Kawazoe Y (2017) Intermolecular interaction in nucleobases and dimethyl sulfoxide/water molecules: A DFT, NBO, AIM and NCI analysis. J Mol Graph Model 78:48–60. https://doi.org/10.1016/j.jmgm.2017.09.022